Z. Phys. C – Particles and Fields 48, 183–190 (1990)

Zeitschrift für Physik C Particles and Fields

Measurement of $K^+ K^-$ production in $\gamma\gamma$ collisions

ARGUS Collaboration

H. Albrecht, H. Ehrlichmann, G. Harder, A. Krüger, A. Nau, A.W. Nilsson, A. Nippe, T. Oest, M. Reidenbach, M. Schäfer, W. Schmidt-Parzefall, H. Schröder, H.D. Schulz, F. Sefkow, R. Wurth
DESY, Hamburg, Federal Republic of Germany

R.D. Appuhn, A. Drescher, C. Hast, G. Herrera, H. Kolanoski, A. Lange, A. Lindner, R. Mankel, H. Scheck, M. Schieber, G. Schweda, B. Spaan, A. Walther, D. Wegener
Institut für Physik [1], Universität, Dortmund, Federal Republic of Germany

M. Paulini, K. Reim, U. Volland, H. Wegener
Physikalisches Institut [2], Universität, Erlangen-Nürnberg, Federal Republic of Germany

W. Funk, J. Stiewe, S. Werner
Institut für Hochenergiephysik [3], Universität, Heidelberg, Federal Republic of Germany

S. Ball, J.C. Gabriel, C. Geyer, A. Hölscher, W. Hofmann, B. Holzer, S. Khan, J. Spengler
Max-Planck-Institut für Kernphysik, Heidelberg, Federal Republic of Germany

D.I. Britton [4], C.E.K. Charlesworth [5], K.W. Edwards [6], H. Kapitza [6], P. Krieger [5], R. Kutschke [5], D.B. MacFarlane [4], K.W. McLean [4], R.S. Orr [5], J.A. Parsons [5], P.M. Patel [4], J.D. Prentice [5], S.C. Seidel [5], G. Tsipolitis [4], K. Tzamariudaki [4], T.-S. Yoon [5]
Institute of Particle Physics [7], Canada

T. Ruf [8], S. Schael, K.R. Schubert, K. Strahl, R. Waldi, S. Weseler
Institut für Experimentelle Kernphysik [9], Universität, Karlsruhe, Federal Republic of Germany

B. Boštjančič, G. Kernel, P. Križan [10], E. Križnič, T. Živko
Institut J. Stefan and Oddelek za fiziko [11], Univerza v Ljubljani, Ljubljana, Yugoslavia

H.I. Cronström, L. Jönsson
Institute of Physics [12], University, Lund, Sweden

A. Babaev, M. Danilov, A. Droutskoy, B. Fominykh, A. Golutvin, I. Gorelov, F. Ratnikov, V. Lubimov, A. Rostovtsev, A. Semenov, S. Semenov, V. Shevchenko, V. Soloshenko, V. Tchistilin, I. Tichomirov, Yu. Zaitsev
Institute of Theoretical and Experimental Physics, Moscow, USSR

R. Childers, C.W. Darden
University of South Carolina [13], Columbia, SC, USA

Received 9 January 1990

[1] Supported by the German Bundesministerium für Forschung und Technologie, under contract number 054DO51P
[2] Supported by the German Bundesministerium für Forschung und Technologie, under contract number 054ER12P
[3] Supported by the German Bundesministerium für Forschung und Technologie, under contract number 054HD24P
[4] McGill University, Montreal, Quebec, Canada
[5] University of Toronto, Toronto, Ontario, Canada
[6] Carleton University, Ottawa, Ontario, Canada
[7] Supported by the Natural Sciences and Engineering Research Council, Canada
[8] Now at ETH Zuerich, Switzerland
[9] Supported by the German Bundesministerium für Forschung und Technologie, under contract number 054KA17P
[10] Supported by Alexander v. Humboldt Stiftung, Bonn
[11] Supported by Raziskovalna skupnost Slovenije and the Internationales Büro KfA, Jülich
[12] Supported by the Swedish Research Council
[13] Supported by the U.S. Department of Energy, under contract DE-AS09-80ER10690

Abstract. The production of charged kaon pairs in two-photon interactions has been studied with the ARGUS detector and the topological cross section has been measured. The $\gamma\gamma$-widths and interference parameters have been determined for the tensor mesons $f_2(1270)$, $a_2(1318)$ and $f_2'(1525)$. The helicity structure assumed for the continuum contribution has a significant effect on the result. Upper limits have been obtained for the $\gamma\gamma$-widths of the glueball candidate states $f_2(1720)$ and $X(2230)$.

Kaon pair production at low masses (1–2 GeV/c^2) in two-photon interactions is expected to contain, in addition to the continuum, contributions from the tensor mesons: $f_2(1270)$, $a_2(1318)$, and $f_2'(1525)$. The helicity structure and relative phases of the production amplitudes of these mesons are not well known experimentally. However, theoretical arguments based on a variety of models [1] show that a ratio of helicity 2 to helicity 0 components of 6:1 or greater is a reliable assumption, with pure helicity 2 being favoured. It is natural to expect interference between the resonance amplitudes and K^+K^- continuum as significant helicity 2 contributions are expected in both [1, 2]. In charged kaon pair production, the relative phases of the three resonances are expected to be zero, while in the production of neutral kaon pairs the f_2: a_2 phase is expected to be 180°. These results require only the weak assumptions of approximate SU(3) flavour symmetry and OZI suppression [3]. Non-$q\bar{q}$ contributions would alter these expectations. In this analysis the continuum interference effect has been taken into account for the first time. The relative phases of the resonances have also been measured for the first time in the charged final state.

The data used in these investigations correspond to an integrated luminosity of 281 pb^{-1}, collected using the ARGUS detector at the e^+e^- storage ring DORIS II at DESY. The beam energies varied between 4.7 and 5.3 GeV. ARGUS is a 4π magnetic spectrometer and is described in detail in [4]. The triggers used for this study required at least two charged particles in the central detector which covers 70% of the solid angle. The transverse momentum threshold for charged particles varied between 0.125 GeV/c and 0.250 GeV/c depending on the event geometry.

Candidate events for the reaction $\gamma\gamma \to K^+K^-$ were selected by requiring two oppositely charged particles in the detector. These had to be traced to within 5 cm of the interaction point along the beam line and 1.5 cm in the transverse plane. The scalar momentum sum of the two particles was required to be less than 4 GeV/c in order to reject events from e^+e^- annihilation. All events containing particles with an ionization energy loss in the drift chamber consistent with that expected from a proton or a more massive particle were rejected. This, together with the vertex constraint, eliminated events from beam gas collisions. No isolated clusters of energy greater than 0.05 GeV were allowed in the electromagnetic calorimeter. Finally, the transverse momentum of each particle was required to be greater than 0.15 GeV/c and the cosine of the angle between each particle's trajectory and the beam was required to be less than 0.7 in magnitude.

The most important aspect of detector performance for this analysis is the charged particle identification. This information was derived from the specific ionization measurement (dE/dx) in the drift chamber and the time of flight (ToF) determination from the scintillation counters. The dE/dx resolution obtained is approximately 6.0%, allowing a pion/kaon separation of more than 3 standard deviations for momenta below 0.8 GeV/c. The ToF system has a resolution of 230 picoseconds, and provides pion/kaon separation of 3 standard deviations for momenta below 0.7 GeV/c. For each charged particle, the particle identification information from each detector element is used to calculate χ^2 values for various mass hypotheses. The dE/dx χ^2 values from both particles in an event are summed and used to calculate a likelihood ratio:

$$P_\alpha = \frac{f_\alpha e^{-\chi_\alpha^2/2}}{\Sigma_\beta f_\beta e^{-\chi_\beta^2/2}},$$
$$(\alpha, \beta = e^+e^-, \mu^+\mu^-, \pi^+\pi^-, K^+K^-, p\bar{p}).$$

The relative abundances, f_α, used were: $f_{e^+e^-}=5.0$, $f_{\mu^+\mu^-}=5.0$, $f_{\pi^+\pi^-}=1.0$, $f_{K^+K^-}=0.04$, $f_{p\bar{p}}=0.01$ These were estimated from previous results in two-photon interactions. The analysis is insensitive to the exact values of these abundances.

It was required that the K^+K^- likelihood ratio, calculated using dE/dx information, be in excess of 0.1%. Events with hits in the muon chambers were rejected. At this point the signal was dominated by background from the two-photon QED final states e^+e^- and $\mu^+\mu^-$. An estimate of this contribution was calculated using the event generator of Daverveldt [5] and the ARGUS full detector simulation [6]. The QED contribution that survived represented a rejection of 40:1 before any ToF information was used. For final state masses above 1.7 GeV/c^2, where no significant contribution from $\gamma\gamma \to \pi^+\pi^-$ is expected, the data were well described by the simulation.

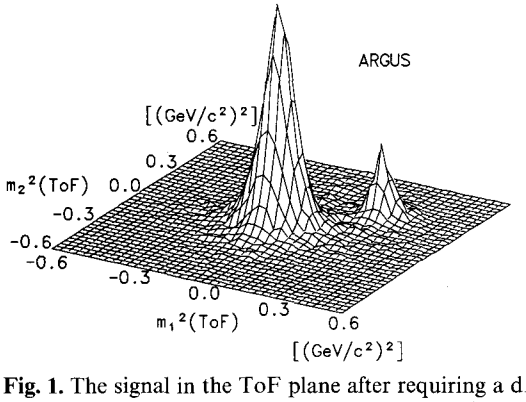

Fig. 1. The signal in the ToF plane after requiring a dE/dx K^+K^- likelihood ratio of at least 0.1%. The axes are the masses squared for each of the two particles in an event as determined from momentum and ToF measurements. Enhancements are seen near the origin (two-photon production of e^+e^-, $\mu^+\mu^-$, and $\pi^+\pi^-$ pairs) and in the region expected to be populated by kaon pair production

The remaining QED background was rejected by making restrictions on the particles masses as derived from the ToF information. A scatter plot of the two m^2_{ToF} from each event is shown in Fig. 1. A clear enhancement is visible around the point $(m^2_{K^+}, m^2_{K^-})$. The 1556 events within a circle of radius 0.15 $(\mathrm{GeV/c^2})^2$ around that point were selected as K^+K^- candidates. The background from pairs of lighter particles was estimated from regions of the same size around the three symmetric points: $(\pm m^2_{K^+}, -m^2_{K^-})$ and $(-m^2_{K^+}, m^2_{K^-})$. Each of these regions should contain approximately equal contributions from the two-photon production of e^+e^-, $\mu^+\mu^-$ and $\pi^+\pi^-$ pairs. The events in these regions were used as a background sample. The average population of these regions is 7 ± 2 events for final state masses less than 1.8 $\mathrm{GeV/c^2}$. The corresponding estimate from the Monte Carlo simulation is 13 ± 7, in good agreement. No significant contribution is expected from $\tau^+\tau^-$ production. An alternate particle identification method, requiring a likelihood ratio of at least 10%, as calculated using the sum of $\mathrm{d}E/\mathrm{d}x$ and ToF χ^2 values, yields consistent results.

The outgoing leptons in the reaction $e^+e^- \to e^+e^-K^+K^-$ are produced predominantly at very small polar angles. The polar angles of these leptons were restricted to be less than 20° by rejecting all events in which they were observed. A cut was made on the transverse momentum of the K^+K^- pair to be less than 0.2 GeV/c to ensure that the photons were nearly real. The average photon q^2 with these cuts is 0.004 $(\mathrm{GeV/c})^2$ and is insensitive to details of the q^2 dependence of the cross section. These requirements also ensure that only the contributions of helicities 0 or 2 need to be included in the analysis. Figure 2 shows the transverse momentum distribution of the selected events, compared to a Monte Carlo estimate using a GVDM propagator [1]; they are in excellent agreement. After the transverse momentum cut, 1262 events remain.

The resulting K^+K^- invariant mass distribution is shown in Fig. 3. The f_2 and a_2 mesons appear as a combined peak and there is a clear signal for the f_2'. Also shown is the QED background distribution, determined as described previously. The QED background is significant only for K^+K^- invariant masses larger than 1.8 $\mathrm{GeV/c^2}$, well above the resonance region under study.

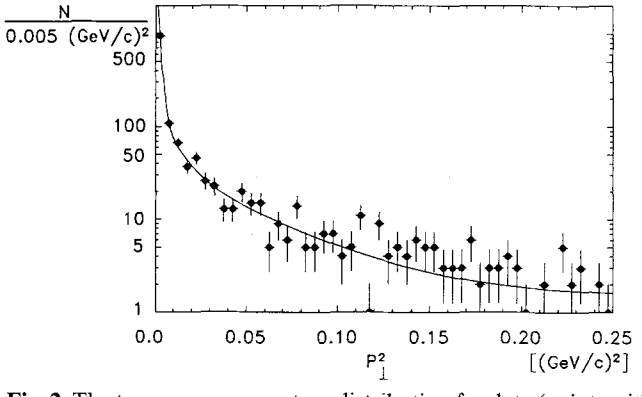

Fig. 2. The transverse momentum distribution for data (points with error bars). The curve shown is the Monte Carlo distribution weighted with the cross section from fit 1B

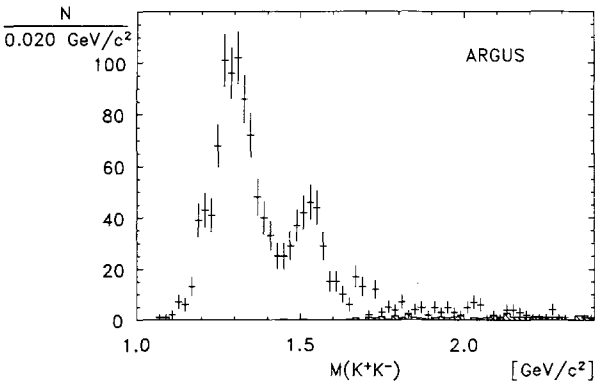

Fig. 3. The invariant K^+K^- mass spectrum after requiring a $\mathrm{d}E/\mathrm{d}x$ K^+K^- likelihood ratio of at least 0.1% and a distance of less than 0.15 $(\mathrm{GeV/c^2})^2$ from the $(m^2_{K^+}, m^2_{K^-})$ point in the ToF plane. The shaded histogram is the background from two-photon QED channels as estimated from similar cuts centered on the points: $(m^2_{K^+}, -m^2_{K^-})$, $(-m^2_{K^+}, m^2_{K^-})$, and $(-m^2_{K^+}, -m^2_{K^-})$

In order to calculate the acceptance, a Monte Carlo program was used to simulate the reaction $e^+e^- \to e^+e^-K^+K^-$. The program used the luminosity functions for transverse photons [7], a constant differential $\gamma\gamma$ cross section, and a beam energy distribution identical to that of the data. The Monte Carlo events (approximately 10^5) were passed through the ARGUS full detector simulation [6] and were reconstructed and analysed using the same programs as were used for experimental data. The simulation of kaon interactions in the electromagnetic calorimeter was derived from ARGUS data on kaons from $\phi(1020)$ and $K^*(892)$ decays. The trigger was also simulated in detail, including variations in logic, thresholds, and other experimental conditions.

To extract information from the data, a maximum-likelihood method is used, avoiding the loss of information inherent in fitting binned distributions. For a parameter set $\vec{\lambda}$, the logarithm of the Poisson likelihood is:

$$L = \sum_{\text{data}} \log \frac{\mathrm{d}\sigma}{\mathrm{d}\cos\theta}(\vec{\lambda}, W^i_{\gamma\gamma}, \cos\theta^i) - \int \frac{\mathrm{d}\sigma}{\mathrm{d}\cos\theta}(\vec{\lambda}, W_{\gamma\gamma}, \cos\theta)\, S(W_{\gamma\gamma}, \cos\theta)\, \mathrm{d}\cos\theta\, \mathrm{d}W_{\gamma\gamma} + \text{terms independent of } \vec{\lambda},$$

where $W^i_{\gamma\gamma}$ and $\cos\theta_i$ are the final state mass and decay angle of the i^{th} event in the data sample. The sensitivity, S, is the number of events expected per nanobarn of differential cross section. The integral was evaluated by Monte Carlo. S is plotted in Fig. 4a(4b) as a function of $W_{\gamma\gamma}(\cos\theta)$. The parameters λ_i (such as resonance masses and widths) can be constrained to the results of previous measurements $(\lambda_i^* \pm \Delta\lambda_i^*)$ by the addition of a term: $-\chi^2(\lambda_i)/2$, where $\chi^2 = (\lambda_i - \lambda_i^*)^2/(\Delta\lambda_i^*)^2$. The likelihood is then maximized and statistical errors (Δ_i) on each parameter are calculated as the change required

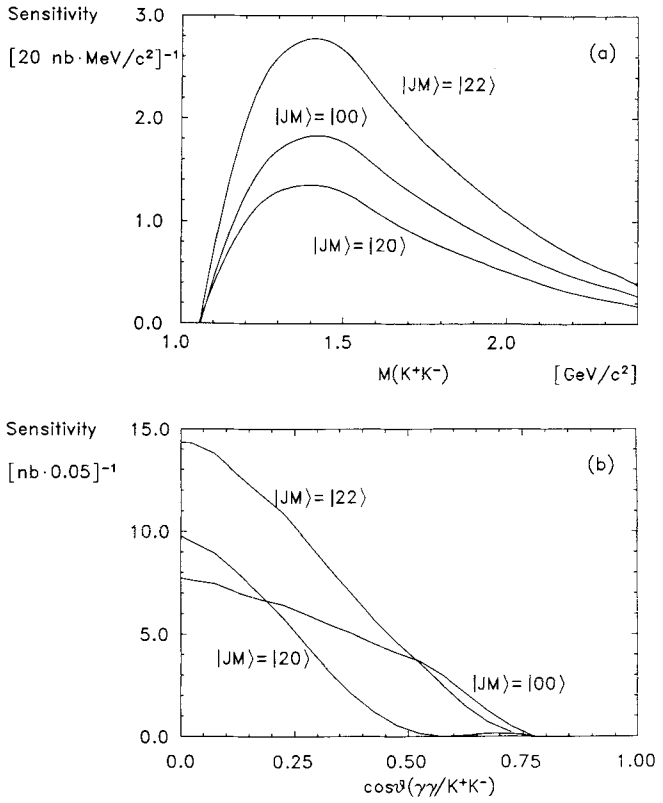

Fig. 4a, b. Sensitivity as a function of (a) $W_{\gamma\gamma}$, and (b) $\cos\theta$ for each partial wave, $JM=22$, 20, and 00

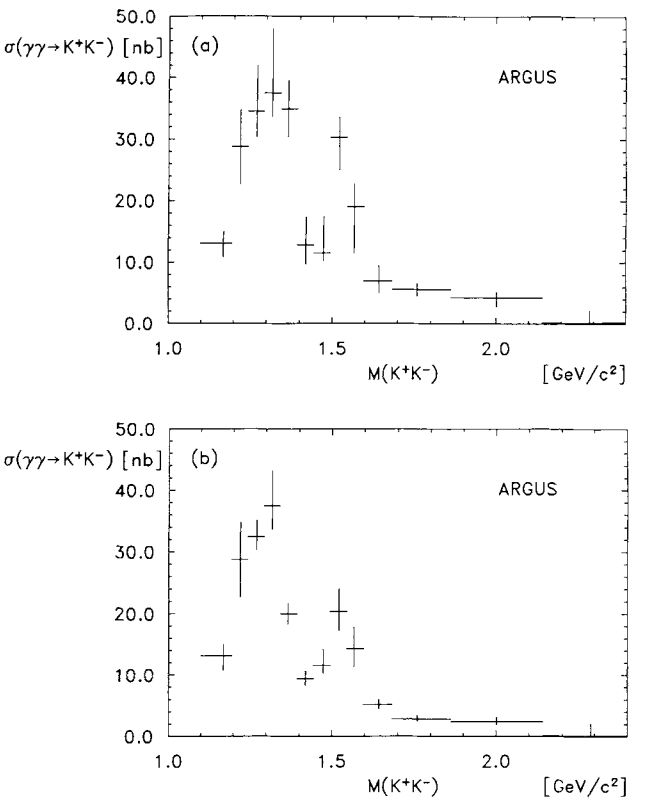

Fig. 5a, b. The cross section for $\gamma\gamma\to K^+K^-$ (errors shown do not include the systematic error of normalization). In **a** contributions from $JM=22$, 20, 00 are allowed, in **b** only $JM=22$, 00 can contribute

to decrease the maximum by 0.5 with all other parameters fixed. In contrast, the change (Δ_i') required to decrease the maximum likelihood by 0.5 with all parameters free is used to calculate the error due to correlations between the parameters: $\Delta_i^{\text{corr}}=\sqrt{\Delta_i'^2-\Delta_i^2}$. This error calculation does not take into account statistical error in the Monte Carlo integral. However, this error is less than 0.7%.

As the q^2 of each colliding photon is small, one can reconstruct the angle, θ, between the $\gamma\gamma$ collision axis and the K^+K^- decay axis by assuming that the photons are collinear with the colliding beams (this has a resolution of 0.007 in $\cos\theta$). Assuming that contributions from angular momenta higher than 2 are negligible, the full angular distribution can be described as:

$$\frac{d\sigma}{d\Omega}=\sigma_{2\pm2}|Y_{22}|^2+\sigma_{20}|Y_{20}|^2+\sigma_{00}|Y_{00}|^2 +2\sqrt{\sigma_{20}\sigma_{00}}|Y_{00}\overline{Y_{20}}|\cos\zeta.$$

The σ_{JM} are cross sections for the partial waves involved while ζ is the relative phase of the 00 and 20 partial waves. As the distributions involved are not linearly independent ($|Y_{20}|=\sqrt{5}|Y_{00}|-\sqrt{6}|Y_{22}|$) one cannot determine all four parameters unambiguously. However, one can still extract the total cross section using a three parameter fit – fixing any one of the four parameters does not restrict the shape of the angular distribution used in the acceptance calculation. The result of this fit is shown in Fig. 5a. If one constrains σ_{20} to be zero (helicity 2 dominance) the cross section in Fig. 5b is obtained. The errors shown are statistical only (the Δ_i' defined above).

The systematic error in the normalization of the cross section is 8.4%. It is composed of contributions due to uncertainties in the particle identification efficiency ($\pm5.0\%$), trigger simulation, event reconstruction and Monte Carlo simulation ($\pm5.7\%$), contributions from QED events ($\pm2.0\%$), and luminosity measurement ($\pm3.0\%$). For K^+K^- invariant masses above 1.8 GeV/c^2, there is an additional uncertainty of $\pm10\%$ from subtraction of the background from QED two-photon processes.

To extract the resonance parameters from the data, we parametrized the cross section as described below. The production, by two real photons, of a single tensor meson with subsequent decay to a K^+K^- pair can be written [1] as:

$$\frac{d\sigma_{\gamma\gamma\to K^+K^-}(W_{\gamma\gamma},\cos\theta)}{d\Omega}=\frac{40\pi}{W_{\gamma\gamma}^2}(|A_0|^2+|A_2|^2)$$

where $W_{\gamma\gamma}$ is the mass of the kaon pair. The helicity 0 and helicity 2 amplitudes are:

$$A_0=\text{BW}(W_{\gamma\gamma})\cdot(W_{\gamma\gamma}/m)^2\cdot(\Gamma_{\gamma\gamma}^{(0)})^{1/2}\cdot Y_{20}(\cos\theta)$$
$$A_2=\text{BW}(W_{\gamma\gamma})\cdot(\Gamma_{\gamma\gamma}^{(2)})^{1/2}\cdot Y_{22}(\cos\theta,\phi).$$

The relativistic Breit-Wigner amplitude is given by:

$$\mathrm{BW}(W_{\gamma\gamma}) = m\sqrt{\Gamma(W_{\gamma\gamma})\cdot \mathrm{Br}(K^+K^-)}/(W_{\gamma\gamma}^2 - m^2 + im\Gamma(W_{\gamma\gamma})).$$

Here m is the mass of the tensor meson and $\Gamma(W_{\gamma\gamma})$ its mass-dependent width:

$$\Gamma(W_{\gamma\gamma}) = \Gamma(m)\cdot(k^*(W_{\gamma\gamma})/k^*(m))^5\cdot(m/W_{\gamma\gamma})\cdot(h(W_{\gamma\gamma})/h(m))$$

where $k^*(W_{\gamma\gamma})$ is the kaon momentum in the tensor meson rest frame and $h(W_{\gamma\gamma})$ is the decay form factor [8], $h(W_{\gamma\gamma}) \propto (9 + 3(k^*r)^2 + (k^*r)^4)^{-1}$. The effective interaction radius, r, is taken as 1 fm. A 10% variation of this parameter affects the values of the two-photon widths at the 2% level. As the product $\Gamma(W)\cdot B(R \to K^+K^-)$ represents the partial width into K^+K^- it should not, in principle, have the same mass dependence as the $\Gamma(W)$ in the denominator of the Breit-Wigner which represents the total width. Introducing the contribution of the known decays of these mesons in the mass dependence of $\Gamma(W)$ affects the results at the 5% level.

As the K^+K^- mass region under investigation is expected to have contributions from three tensor mesons, $f_2(1270)$, $a_2(1318)$, and $f_2'(1525)$, interference between them must be included. The continuum K^+K^- amplitudes (G_M) are also expected to interfere. This leads to the total amplitude for $\gamma\gamma \to K^+K^-$ for helicity M(0 or 2) to be:

$$T_M = A_M(f_2) + \exp(i\phi_{f_2:a_2})\cdot A_M(a_2) + \exp(i\phi_{f_2:f_2'}) \cdot A_M(f_2') + \exp(i\phi_M)\cdot G_M.$$

The two phases $\phi_{f_2:a_2}$ and $\phi_{f_2:f_2'}$ represent the interference between the resonances while the ϕ_M are the overall phase differences between the resonances and continuum.

As the data sample is too small for a complete analysis, certain assumptions had to be made. The most critical of these involve the continuum contribution, the functional form of which is unknown: The results presented below are averages of the results of several fits using different continuum parametrizations (e.g. third order polynomial with threshold factor; Born terms [1] with a free complex coefficient for each helicity contribution). Only those parametrizations that yield reasonable likelihoods are used. The systematic error for each result is the sum in quadrature of the standard deviation of the results from the good continuum parametrizations, the error from correlations (Δ_i^{corr} as described above, these are dominated by contributions from the parameters describing the continuum) and the systematic error from normalization.

Ideally, the continuum should also have a phase for each helicity that varies with the mass of the kaon pair. However, the assumption was made that the continuum phase is constant. To further simplify the analysis it was assumed that the continuum is either entirely coherent ($\{JM\} = \{22\}$) or incoherent ($\{JM\} = \{00\}$) except in the case of fits using a modified Born term. In this parametrization the Born term contribution for each helicity was scaled by a complex constant. However, the magnitude of the helicity 0 scale factor was consistently less than 5%. One should note that this is the first analysis to be even this general. Previous analyses of the K^+K^- final state assumed an incoherent continuum [9–12], while studies of the $K_S^0\,\bar{K}_S^0$ final state [13, 14] assumed no continuum contribution. The incoherent continuum hypothesis has a smaller likelihood and was included principally to demonstrate consistency with the results of previous measurements that made this assumption. The masses and widths of the resonances involved were constrained to the world average values [15].

To study the 8 parameters describing the amplitudes T_M, the cross section parametrization discussed above was fitted to the data corresponding to the mass spectrum in Fig. 3. The results, for various hypotheses, are shown in the tables which also summarize the assumptions for each fit. In fit 1 A, the f_2 and a_2 contributions are free and the results are determined using a coherent continuum:

$$\Gamma_{\gamma\gamma}(f_2)\cdot \mathrm{Br}(f_2 \to K\bar{K}) = (0.104 \pm 0.007 \pm 0.072)\ \mathrm{keV}$$
$$\Gamma_{\gamma\gamma}(a_2)\cdot \mathrm{Br}(a_2 \to K\bar{K}) = (0.081 \pm 0.006 \pm 0.027)\ \mathrm{keV}$$

Table 1a. Two-photon widths from fits with a coherent continuum. Entries without errors are fixed in the corresponding fits, while values in parentheses are used as constraints. More details of the fits are given in Table 1b

Fit	$\Gamma_{\gamma\gamma}\cdot B(K\bar{K})$ [eV]			
	f_2	a_2	f_2', $JM=22$	f_2', $JM=20$
1 A	$104.0 \pm 7.0 \pm 72.0$	$81.0 \pm 6.0 \pm 27.0$	$35.7 \pm 5.5 \pm 9.6$	0
1 B	$\left(130.0^{+34.0}_{-24.0}\right)$	(48.0 ± 10.0)	$31.4 \pm 5.0 \pm 7.7$	0
1 C	$\left(130.0^{+34.0}_{-24.0}\right)$	(48.0 ± 10.0)	$32.3 \pm 4.9 \pm 8.8$	0
1 D	$\left(130.0^{+34.0}_{-24.0}\right)$	(48.0 ± 10.0)	$33.4 \pm 5.6 \pm 11.3$	0
1 E	$\left(130.0^{+34.0}_{-24.0}\right)$	(48.0 ± 10.0)	$27.7 \pm 7.6 \pm 9.3$	$45.0 \pm 6.8 \pm 43.8$
1 F	$\left(130.0^{+34.0}_{-24.0}\right)$	(48.0 ± 10.0)	$26.2 \pm 7.3 \pm 8.7$	$48.5 \pm 7.0 \pm 42.7$

Table 1b. Phases from fits with a coherent continuum. Entries without errors are fixed in the corresponding fits. The two photon widths obtained from the fits are given in Table 1a

Fit	Relative phases [degrees]			Log likelihood
	$\phi_{f_2:a_2}$	$\phi_{f_2:f_2'}$	ϕ_2	
1 A	0	0	$-122\pm 7\pm 14$	66.9
1 B	0	0	$-116\pm 9\pm 14$	65.8
1 C	0	$-5\pm 5\pm 15$	$-91\pm 14\pm 27$	66.1
1 D	$30\pm 12\pm 24$	$32\pm 13\pm 26$	$-126\pm 8\pm 14$	66.3
1 E	0	0	$-108\pm 8\pm 17$	66.0
1 F	0	$-2\pm 5\pm 22$	$-121\pm 14\pm 28$	66.3

where 0° phase difference between the resonances and helicity 2 dominance were assumed. The result is consistent with the world average values [15, 16]:

$$\Gamma_{\gamma\gamma}(f_2)\cdot \mathrm{Br}(f_2\to K\bar{K}) = \left(0.130\,^{+0.034}_{-0.024}\right)\mathrm{keV}$$

$$\Gamma_{\gamma\gamma}(a_2)\cdot \mathrm{Br}(a_2\to K\bar{K}) = (0.048\pm 0.010)\,\mathrm{keV}$$

as demonstrated by the likelihood decrease of 1.1 on introducing these world averages as constraints in fit 1 B. The unconstrained results in the incoherent case (fig 2 A) are:

$$\Gamma_{\gamma\gamma}(f_2)\cdot \mathrm{Br}(f_2\to K\bar{K}) = (0.091\pm 0.007\pm 0.027)\,\mathrm{keV}$$

$$\Gamma_{\gamma\gamma}(a_2)\cdot \mathrm{Br}(a_2\to K\bar{K}) = (0.126\pm 0.007\pm 0.028)\,\mathrm{keV}.$$

There is a likelihood decrease of 2.0 on imposing the world average values as constraints (fit 2 B), demonstrating that the incoherent continuum ansatz is less consistent with the known $\Gamma_{\gamma\gamma}$ values for the f_2 and a_2 than a coherent continuum. Together with a likelihood difference of more than 10 between the coherent and incoherent fits with the f_2 and a_2 constrained, this provides strong evidence of a coherent contribution in addition to the resonances. Unfortunately, the quality of the results for the f_2 and a_2 mesons was limited by the difficulty of separating the two merged resonances, and by the uncertainty in the continuum contribution. Due to this, the contributions of these two resonances were constrained to the world averages [15, 16] to study the f_2' with less uncertainty from the continuum.

The most striking effect of the coherent continuum is a suppression of the $\gamma\gamma$-width of the f_2' by approximate-

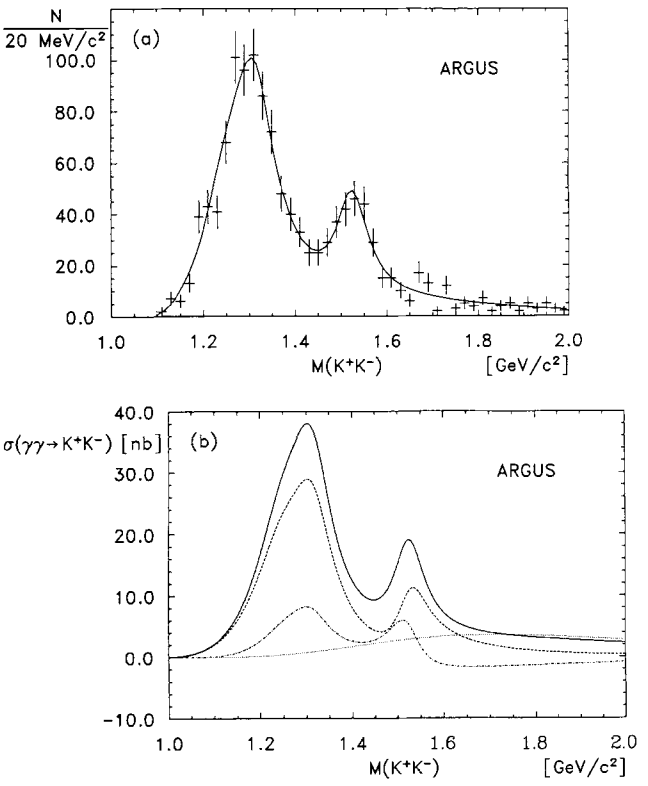

Fig. 6a, b. Results of fit 1 B (errors shown are statistical). In **a** the curve is the fitted cross section convoluted with sensitivity while the points with error-bars are from data; **b** shows the fitted cross sections: total (solid line), resonant (dashed), interference term (dot-dashed), and continuum (dotted)

Table 2a. Two-photon widths from fits with an incoherent continuum. Entries without errors are fixed in the corresponding fits, while values in parentheses are used as constraints. More details of the fits are given in Table 2b

Fit	$\Gamma_{\gamma\gamma}\cdot B(K\bar{K})$ [eV]			
	f_2	a_2	$f_2', JM=22$	$f_2', JM=20$
2 A	$91.0\pm 7.0\pm 27.0$	$126.0\pm 7.0\pm 28.0$	$74.9\pm 8.5\pm 14.8$	0
2 B	$\left(130.0\,^{+34.0}_{-24.0}\right)$	(48.0 ± 10.0)	$67.3\pm 8.1\pm 15.1$	0
2 C	$\left(130.0\,^{+34.0}_{-24.0}\right)$	(48.0 ± 10.0)	$57.5\pm 6.7\pm 12.7$	0
2 D	$\left(130.0\,^{+34.0}_{-24.0}\right)$	(48.0 ± 10.0)	$57.9\pm 7.4\pm 12.1$	0
2 E	$\left(130.0\,^{+34.0}_{-24.0}\right)$	(48.0 ± 10.0)	$28.7\pm 9.0\pm 10.2$	$121.0\pm 13.1\pm 31.6$
2 F	$\left(130.0\,^{+34.0}_{-24.0}\right)$	(48.0 ± 10.0)	$35.7\pm 8.7\pm 11.7$	$80.1\pm 9.1\pm 38.2$

Table 2b. Phases from fits with an incoherent continuum. Entries without errors are fixed in the corresponding fits. The two photon widths obtained from the fits are given in Table 2a

Fit	Relative phases [degrees]		Log likelihood
	$\phi_{f_2:a_2}$	$\phi_{f_2:f_2'}$	
2 A	0	0	56.6
2 B	0	0	54.6
2 C	0	$27\pm 6\pm 11$	56.4
2 D	$16\pm 10\pm 10$	$40\pm 10\pm 17$	56.4
2 E	0	0	57.1
2 F	0	$22\pm 10\pm 15$	57.5

ly 50% with respect to the incoherent case. The interference term is of the form $A\cos(\phi_R-\phi_2)$ where ϕ_R varies from $-\pi$ to 0 in a counterclockwise sense on traversing the resonance. However, ϕ_2 is determined to be close to $-\pi/2$, so the integral of the interference term is positive. The main effect of the interference term is to change the resonance shape (Fig. 6b). In fits E and F an additional incoherent $\{JM\}=\{20\}$ term is allowed. A large effect is seen because of the absence of interference and the lower sensitivity to helicity 0 contributions.

The preferred value for the strenght of f_2' production in two-photon interactions is:

$$\Gamma_{\gamma\gamma}(f_2')\cdot \mathrm{Br}(f_2'\to K\bar{K})=(0.0314\pm 0.0050\pm 0.0077)\ \mathrm{keV}$$

with the assumptions of helicity 2 dominance, 0° phase relative to the $f_2(1270)$, and a coherent continuum contribution (fit 1 B). The result of fit 1 B is illustrated in Fig. 6. This is to be compared to the current world average value [16] of (0.09 ± 0.02) keV. It should be emphasized again that, in all the experiments contributing to this value, the continuum was taken to be incoherent with respect to the resonance production. With an incoherent continuum contribution the result becomes:

$$\Gamma_{\gamma\gamma}(f_2')\cdot \mathrm{Br}(f_2'\to K\bar{K})=(0.0673\pm 0.0081\pm 0.0151)\ \mathrm{keV}$$

again with helicity 2 dominance and 0° resonance phase (fit 2 B).

The relative phases of the resonances are consistent with zero as expected. The results with a coherent continuum (fit 1 D) are:

$$\phi_{f_2:a_2}=(30\pm 12\pm 26)°$$
$$\phi_{f_2:f_2'}=(32\pm 13\pm 26)°.$$

In this fit the magnitudes of the f_2 and a_2 contributions are constrained to their world averages and helicity 2 dominance is assumed.

There have been many attempts [17–23] to calculate tensor meson $\gamma\gamma$-widths. The present measurement, taken together with the world average values for the f_2 and a_2, and assuming that $50\%<\mathrm{Br}(f_2'\to K\bar{K})<100\%$, is consistent only with one model [21]. This agreement is improved if one takes into account recent data on f_2' decays to K^+K^-, $\pi^+\pi^-$, and $\eta\eta$ observed in J/ψ decays [24] which yield a value for the branching ratio of $\mathrm{Br}(f_2'\to K\bar{K})=\left(72\,^{+7}_{-13}\right)\%$, assuming that no other decay modes contribute.

Assuming $\mathrm{Br}\ (f_2'\to K\bar{K})=100\%$, this measurement of $\Gamma_{\gamma\gamma}(f_2')$ can be combined with the world averages of $\Gamma_{\gamma\gamma}(a_2)=(0.98\pm 0.13)$ keV and $\Gamma_{\gamma\gamma}(f_2)=(3.10\pm 0.33)$ keV [16] to obtain the tensor nonet flavour SU(3) mixing parameters [1]:

$$\Gamma_{\gamma\gamma}(f_2'/\Gamma_{\gamma\gamma}(a_2)=\frac{1}{3}(\cos\theta_T-r_T\,2\sqrt{2}\sin\theta_T)^2\left(\frac{m(f_2')}{m(a_2)}\right)^N$$

$$\Gamma_{\gamma\gamma}(f_2)/\Gamma_{\gamma\gamma}(a_2)=\frac{1}{3}(\sin\theta_T+r_T\,2\sqrt{2}\cos\theta_T)^2\left(\frac{m(f_2)}{m(a_2)}\right)^N$$

where $N=3$, -1, or -4 depending on the nature of the production mechanism. Using fit 1B, with $N=3$, leads to values for the singlet/octet mixing angle $\theta_T=(22.2\pm 1.8)°$ and the nonet symmetry breaking parameter $r_T=1.10\pm 0.10$, while with $N=-4$ the results are: $\theta_T=(28.5\pm 2.3)°$, and $r_T=0.96\pm 0.09$, which is consistent with $\theta_T=28°$ as expected from the quadratic mass formula [15]. The largest experimental uncertainty in the determination of these parameters is now associated with the uncertainties of the relatively large $\gamma\gamma$-widths of the f_2 and a_2 mesons.

The $f_2(1720)$ (formerly $\theta(1690)$) is now a well established resonance [15] and is considered a glueball candidate [25]. Due to this, limits on its $\gamma\gamma$-width are of interest. Current theoretical estimates [26] suggest that $\Gamma(f_2(1720)\to\gamma\gamma)\cdot\mathrm{Br}(f_2(1720)\to K\bar{K})$ should be approximately 95 eV, which is close to current experimental sensitivities. Helicity 2 dominance is also expected in $f_2(1720)$ production. The matrix element for the $f_2(1720)$ was introduced into the cross section allowing interference with the other contributions. The mass and width of the $f_2(1720)$ were constrained [25] to be $(1.707\pm 0.011)\ \mathrm{GeV/c^2}$ and $(0.162\pm 0.025)\ \mathrm{GeV/c^2}$ respectively. In addition to the $f_2(1720)$ parameters, only the f_2' $\gamma\gamma$-width, the relative f_2':$f_2(1720)$ phase, and the continuum parameters were free in the fit (all other parameters were as in fit 1B). The likelihood was maximized for different hypothetical values of $\Gamma(f_2(1720)\to\gamma\gamma)\cdot\mathrm{Br}(f_2(1720)\to K\bar{K})$, and the resulting distribution integrated. This leads to the results:

$$\frac{\Gamma_{\gamma\gamma}^{(2)}}{0.058}+\frac{\Gamma_{\gamma\gamma}^{(0)}}{0.24}<\frac{1.0\ \mathrm{keV}}{\mathrm{Br}(f_2(1720)\to K\bar{K})}\ \text{at 95\% c.l.}$$

The $f_2(1720)$ helicity 0 upper limit is much weaker due to the reduced acceptance (approximately a factor of two smaller) and the helicity 2 assumption for all the other contributions. The above analysis employed a coherent continuum contribution.

The $X(2230)$ is less well established than the $f_2(1720)$ but is also considered a glueball candidate. No events are observed in the relevant mass region between 2.21 and 2.25 $\mathrm{GeV/c^2}$ leading to the result:

$$\frac{\Gamma_{\gamma\gamma}^{(2)}}{0.019}+\frac{\Gamma_{\gamma\gamma}^{(0)}}{0.043}<\frac{1.0\ \mathrm{keV}}{\mathrm{Br}(X(2230)\to K\bar{K})}\ \text{at 95\% c.l.}$$

assuming that $J_{PC}=2^{++}$ for the $X(2230)$. This is in agreement with a likelihood analysis using the mass region between 1.8 and 2.4 GeV with the mass and width of the $X(2230)$ constrained to be 2.227 ± 0.008 GeV/c^2 and 0.021 ± 0.018 GeV/c^2 respectively. Theoretical expectations [26] are on the order of 1 eV if the $X(2230)$ is a 2^{++} glueball state.

In summary, the reaction $\gamma\gamma\to K^+K^-$ has been analysed in detail. Cross sections have been determined for this process with minimal assumptions. Production of the tensor mesons f_2, a_2, and f_2' has been observed. Assuming helicity 2 dominance and fixing the phases between the resonances to be zero the strength of f_2' production was found to be $\Gamma_{\gamma\gamma}(f_2')\cdot \mathrm{Br}(f_2'\to K\bar{K})=(0.031\pm0.005\pm0.008)$ keV, with a coherent continuum hypothesis or $(0.067\pm0.008\pm0.015)$ keV with an incoherent continuum. The coherent case is found to have a significantly higher likelihood. The relative phases f_2: a_2 and f_2:f_2' have been determined for the first time in the charged kaon final state and are found to be $(30\pm12\pm24)°$ and $(32\pm13\pm26)°$, consistent with zero. No evidence for production of the glueball candidate states $f_2(1720)$ and $X(2230)$ is observed. With no assumptions on helicity content and with arbitrary phases between the states involved, the following upper limits were determined: $\Gamma_{\gamma\gamma}(f_2(1720))\cdot\mathrm{Br}(f_2(1720)\to K^+K^-)<0.24$ keV and $\Gamma_{\gamma\gamma}(X(2230))\cdot\mathrm{Br}(X(2230)\to K^+K^-)<0.043$ keV with 95% confidence.

Acknowledgements. It is a pleasure to thank U. Djuanda, E. Konrad, E. Michel, and W. Reinsch for their competent technical help in running the experiment and processing the data. We thank Dr. H. Nesemann, B. Sarau, and the DORIS group for the excellent operation of the storage ring. The visiting groups wish to thank the DESY directorate for the support and kind hospitality extended to them.

References

1. H. Kolanoski: Springer Tracts in Modern Physics, vol. 105. Berlin Heidelberg New York: 1984; M. Poppe: Int. J. Mod. Phys. A1 (1986) 545; Ch. Berger, W. Wagner: Phys. Rep. 146C (1987) 1
2. S.J. Brodsky, G.P. Lepage: Phys. Rev. D24 (1981) 1808
3. D. Faiman, H.J. Lipkin, H.R. Rubinstein: Phys. Lett. 59B (1975) 269
4. H. Albrecht et al. (ARGUS): Nucl. Instrum. Methods A275 (1989) 1
5. F.A. Berends, P.H. Daverveldt, R. Kleiss: Nucl. Phys. B253 (1985) 441
6. H. Gennow: DESY F15-85-02 (1985)
7. V.M. Budnev, I.F. Ginzburg, G.V. Meledin, V.G. Serbo: Phys. Rep. 15C (1975) 181
8. K.M. Blatt, V.F. Weisskopf: Theoretical nuclear physics, pp. 359–365; pp. 386–389. New York: Wiley 1952
9. M. Althoff et al. (TASSO): Phys. Lett. 121B (1983) 216
10. H. Aihara et al. (TPC/2γ): Phys. Rev. Lett. 57 (1986) 404
11. G. Gidal (MARK II), VIIth International Workshop on Photon-Photon Collisions. A. Courau, P. Kessler (eds.) p. 418. Paris (1986)
12. R. Johnson (DELCO): Ph. D. Thesis, SLAC-Report 294 (1986)
13. Ch. Berger et al. (PLUTO): Z. Phys. C – Particles and Fields 37 (1988) 329
14. H.J. Behrend et al. (CELLO): Z. Phys. C – Particles and Fields 43 (1989) 91
15. Particle Data Group: Review of Particle Properties: Phys. Lett. 204B (1988) 1
16. S. Cooper: Ann. Rev. Nucl. Part. Phys. 38 (1988) 705
17. H. Suura, T. Walsh, B. Young: Lett. Nuovo Cimento 4 (1972) 505
18. J. Babcock, J.L. Rosner: Phys. Rev. D14 (1976) 1286
19. V.M. Budnev, A.E. Kaloshin: Phys. Lett. 86B (1979) 351
20. P. Singer: Phys. Lett. 124B (1983) 531
21. S. Godfrey, N. Isgur: Phys. Rev. D32 (1983) 189; T. Barnes: VIIth International Workshop on Photon-Photon Collisions. A. Courau, P. Kessler (eds.) p. 28. Paris: (1986)
22. S.B. Berger, B.T. Feld: Phys. Rev. D8 (1973) 3875
23. L. Bergstroem et al.: Z. Phys. C – Particles and Fields 16 (1983) 263
24. L. Köpke, N. Wermes: J/ψ Decays. Phys. Rep. 174 (1989) 67
25. D.G. Hitlin: Invited talk presented at the BNL Workshop on Glueballs, Hybrids, and Exotic Hadrons, p. 88. Upton (1988)
26. E.H. Kada, P. Kessler, J. Parisi: Phys. Rev. D39 (1989) 2657